

A novel quantum machine learning classifier to search for new physics

Ji-Chong Yang,^{*} Shuai Zhang, and Chong-Xing Yue[†]

Department of Physics, Liaoning Normal University, Dalian 116029, China and

Center for Theoretical and Experimental High Energy Physics,

Liaoning Normal University, Dalian 116029, China

(Dated: October 25, 2024)

arXiv:2410.18847v1 [hep-ph] 24 Oct 2024

Abstract

Due to the success of the Standard Model (SM), it is reasonable to anticipate that, the signal of new physics (NP) beyond the SM is small, and future searches for NP and precision tests of the SM will require high luminosity collider experiments. Moreover, as the precision tests of the SM advances, rarer processes with a greater number of final-state particles will require consideration, which will in turn require the analysis of a multitude of observables. As an inherent consequence of the high luminosity, the generation of a large amount of experimental data in a large feature space presents a significant challenge for data processing. In recent years, quantum machine learning has emerged as a promising approach for processing large amounts of complex data on a quantum computer. In this study, we propose a variational quantum searching neighbor (VQSN) algorithm to search for NP. As an example, we apply the VQSN in the phenomenological study of the gluon quartic gauge couplings (gQGCs) at the Large Hadron Collider. The results suggest that VQSN demonstrates superior efficiency to a classical counterpart k-nearest neighbor algorithm, even when dealing with classical data.

I. INTRODUCTION

The standard model (SM) is supported by a substantial body of experimental evidence and can be concluded to describe and explain the majority of phenomena in particle physics, with a few rare exceptions [1–9]. Consequently, there is a widely held belief in the existence of new physics (NP) beyond the SM, and the search for NP and precision tests of the SM have become a prominent area of interest within the high-energy physics (HEP) community [10]. Given the success of the SM, it is reasonable to posit that any NP signals that have yet to be discovered will be exceedingly small. Therefore, the search of NP and the precision tests of the SM motivate higher luminosity collider experiments. The processing of large amounts of data is inherent to such experiments, and thus places demands on our ability to process large amounts of data efficiently.

The application of machine learning (ML) algorithms represents a promising avenue for the efficient processing of data. Its applications have already been demonstrated in HEP [11–

* yangjichong@lnnu.edu.cn

† cxyue@lnnu.edu.cn; Corresponding author

36]. In phenomenological studies of NP, using an ML method usually obviates the necessity for an analysis of the kinematics, therefore, the more complex and challenging to analyze the kinematics, the more evident the benefits of ML become. Consequently, the advantages will become increasingly apparent as further advances in the precision tests of the SM will inevitably involve the study of rare processes with larger numbers of particles in the final states.

In the meantime, quantum computing represents another effective approach for processing large volumes of data. Despite the current status of quantum computing as a noisy intermediate-scale quantum (NISQ) technology [37–39], there has been a notable increase in research activity within the HEP community related to this field [40–59]. Many ML algorithms can be implemented by quantum computing [60–62]. In conjunction with the advancement of quantum ML algorithms, there has been a growing interest in the deployment of quantum ML in the HEP phenomenological studies, encompassing techniques such as variational quantum classifier (VQC) [63–66], quantum support vector machine (QSVM) [63, 67–69], and quantum kernel k-means (QKKM) [70], etc. In this study, we propose a variational quantum searching neighbor (VQSN) algorithm for identifying NP signals.

To illustrate our algorithm, the gluon quartic gauge couplings (gQGCs) [71–73] in the SM effective field theory (SMEFT) [74–77] are considered as the arena. One of the reasons SMEFT has recently been widely used in NP phenomenological research is efficiency [35]. So the choice of gQGCs is in line with the theme of high efficiency. It is found that, in the search of the gQGCs at the large hadron collider (LHC), VQSN is able to demonstrate superior efficiency compared to a classical k-nearest neighbor (KNN) algorithm, even when applied to classical datasets.

II. THE CIRCUIT TO SEARCH THE NEIGHBORS

A circuit can be constructed to find the vectors with higher probabilities for closer neighbors. The first step is to construct $|\psi_n\rangle_a|n\rangle_b$ which can be realized using amplitude encode, the subscript ‘a’ and ‘b’ represent registers for clarity. When the $|\psi_n\rangle_a|n\rangle_b$ state is created, applying on the a register the inverse of a circuit to amplitude encode $|\phi\rangle_a$. And then deduct measurements on a register, when $|0\rangle$ is measured, the state obtained is then $|0\rangle_a \sum_n \langle \phi | \psi_n \rangle |n\rangle$. The success rate to create the state is $\sum |\langle \phi | \psi_n \rangle|^2 / N$, where N is the

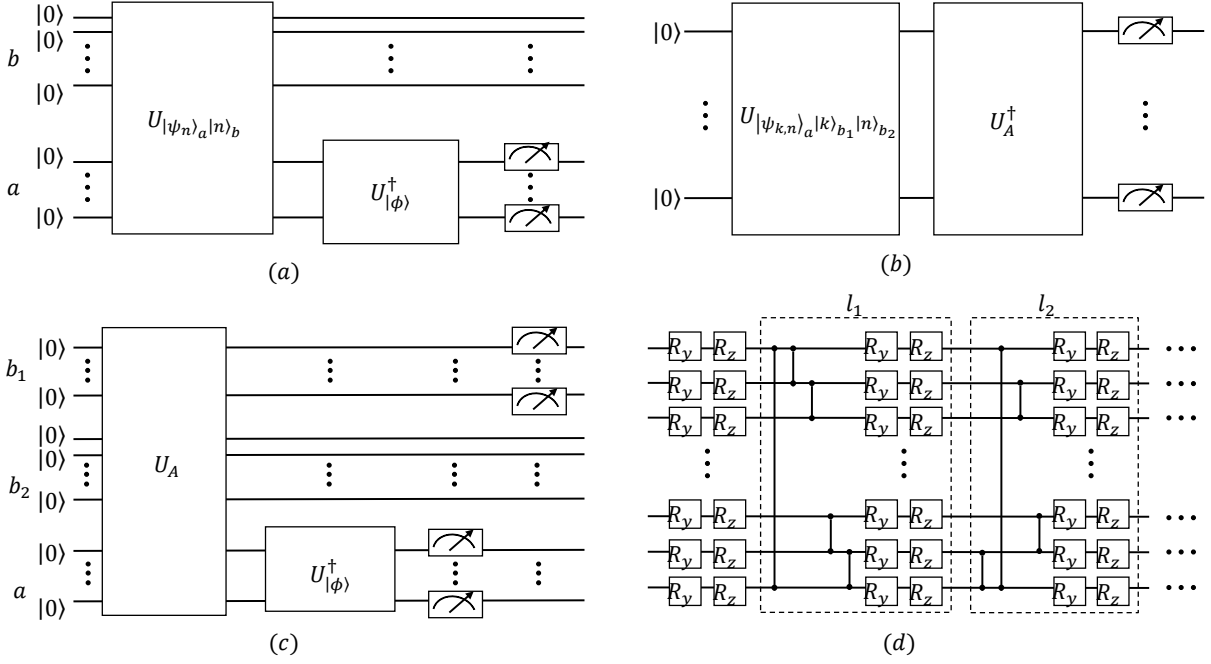


FIG. 1. The circuits used in this work. The top left panel shows the circuit to construct $\langle\phi|\psi_n\rangle|n\rangle$. The top right panel shows the circuit to fit the ansatz. The bottom left panel shows the circuit to find the classification assignment of $|\phi\rangle$. The bottom right panel shows the ‘hardware efficient’ ansatz.

number of ψ_n vectors. Without assumptions on the distribution of the vectors, the success rate is approximately $1/d$ for d -dimensional complex vectors, which is verified by using complex uniform random numbers. The success rate can be improved to $1/\sqrt{d}$ by amplitude amplification, or the ‘QSearch’ algorithm [78].

When $|0\rangle_a \sum_n \langle\phi|\psi_n\rangle|n\rangle_b$ is obtained, a measurement on b register will result in n with the probability proportional to $|\langle\phi|\psi_n\rangle|^2$, therefore, $|n\rangle$ will be obtained with higher probabilities if ψ_n are closer to ϕ . Denoting the amplitude encode circuits as $U_{|\psi_n\rangle|n\rangle}$ and $U_{|\phi\rangle}$, i.e., $U_{|\psi_n\rangle|n\rangle}|0\rangle = |\psi_n\rangle|n\rangle$ and $U_{|\phi\rangle}|0\rangle = |\phi\rangle$, a summary of the circuit to create $\langle\phi|\psi_n\rangle|n\rangle$ is depicted in Fig. 1. (a). Since our goal is to classify, in the following, we assume that the ψ vectors have classification labels and that ψ_n are stored according to the classifications, i.e., the state to be amplitude encoded is $|\psi_{k,n}\rangle_a|k\rangle_{b_1}|n\rangle_{b_2}$, where k denotes the classification assignment.

For classical datasets, an improvement is to fit the state $|\psi_{k,n}\rangle_a|k\rangle_{b_1}|n\rangle_{b_2}$ using an ansatz.

Denoting the circuit of the ansatz as $U_A(\alpha_i)$ where α_i are trainable parameters, the circuit of fitting is shown in Fig. 1. (b), where the probability of the outcome $|0\rangle$ in the measurements is $|\langle \Psi(\alpha_i) | \psi_{k,n} \rangle_a |k\rangle_{b_1} |n\rangle_{b_2}|^2$ with $U_A(\alpha_i)|0\rangle = |\Psi(\alpha_i)\rangle$. The fitting is to find values of parameters α_i to maximize the probability of the outcome $|0\rangle$ in the measurements.

III. VARIATION QUANTUM SEARCHING NEIGHBOR ALGORITHM

To summarize, the steps of the VQSN are listed as follows.

1. Arrange the training dataset as $|\psi_{k,n}\rangle_a |k\rangle_{b_1} |n\rangle_{b_2}$, where k is the class of $\psi_{k,n}$, n is the index of $\psi_{k,n}$ in class k .
2. Using an ansatz $|\Psi(\alpha_i)\rangle$ to fit $|\psi_{k,n}\rangle_a |k\rangle_{b_1} |n\rangle_{b_2}$.
3. For a test vector ϕ , apply the inverse of amplitude encode for $|\phi\rangle_a$ after the ansatz circuit, and measure a register. If $|0\rangle_a$ is measured, the state is successfully created. Apply amplitude amplification if necessary.
4. Measure the b_1 register to find out the classification. Repeat c times and designate the classification of ϕ on the outcomes.

In the case of QSN the step-2 is omitted. The circuit of VQSN is shown in Fig. 1. (c). Since the search of NP is binary, we employ $\hat{a} = a/c$ to quantify whether the ϕ is a signal, where a is the number of times the measurement on b_1 results in a signal. Then we select events with $\hat{a} > \hat{a}_{th}$. In this work, we use $c = 100$.

Given the similarity between the principles of QSN and KNN, a comparison between the two is warranted. Similarly, a tunable KNN (t-KNN) is devised, which employs $\hat{b} = b/K$ to quantify whether a vector is a signal, where b represents the number of signals present in the K nearest neighbors to the vector. Then we select events with $\hat{b} > \hat{b}_{th}$. When $\hat{b}_{th} = 0.5$, t-KNN becomes KNN.

In essence, the VQSN is one of the VQC algorithm. However, it possesses two advantages. Firstly, conventional VQC can be considered as the quantum analogue of an artificial neural network, which is a ‘black box’ difficult to interpret. In contrast, the state to build in QSN has a discernible geometric interpretation, and the target of the training is guaranteed to

exist. Secondly, VQSN is accompanied by a classical algorithm, KNN, which allows for a comparison between quantum and classical algorithms.

For the (t-)KNN algorithm, we only incorporate the cost needed to compute the distances, so the computational complexity (cc) can be estimated as $\mathcal{O}(dNM)$ for M test events. In the context of quantum computers, the number of quantum gates is typically employed as a means of assessing the cc. Even if the dataset is classical, the cc for VQSN is $n_t + \mathcal{O}(cN(n_{ans} + d)\sqrt{d})$, where n_t is the cost to train the ansatz which is a constant in the view of test dataset, n_{ans} is the cc of the ansatz, the cc of $U_{|\phi\rangle}^\dagger$ is $\mathcal{O}(d)$, and the $\mathcal{O}(\sqrt{d})$ comes from the success rate to create the state $\langle\phi|\Psi(\alpha_i)\rangle$. With a large M , it can be roughly estimated that the VQSN outperforms (t-)KNN when $c(n_{ans} + d) < N\sqrt{d}$. From the principle of the algorithm, the larger N and d , the better the classification, which means that ideally VQSN can outperform (t-)KNN even dealing with a classical dataset.

IV. SEARCH OF THE GLUON QUARTIC GAUGE COUPLINGS

In the SMEFT, the operators contributing to gQGCs appear at dimension-8. We focus on the $O_{gT,0}$ operator,

$$O_{gT,0} = \frac{1}{16M_0^4} \sum_a G_{\mu\nu}^a G^{a,\mu\nu} \times \sum_i W_{\alpha\beta}^i W^{i,\alpha\beta}, \quad (1)$$

where $G_{\mu\nu}^a$ is gluon field strengths, $W_{\mu\nu}^i$ denote electroweak field strengths, and M_0 is the NP scale. The expected constraints is $M_0 \geq 1040$ MeV at the LHC with the center of mass (c.m.) energy $\sqrt{s} = 13$ TeV, and luminosity $L = 36.7$ fb $^{-1}$ obtained by using the process $gg \rightarrow \gamma\gamma$ [71]. For convenience, we define $f_0 \equiv 1/(16M_0^4)$.

ML algorithms are more suitable for processes with more intricate final states, which necessitates greater investment in kinematic analysis when traditional methods are employed. In this work, we consider three processes $pp \rightarrow j\ell^+\ell^-\bar{\nu}\nu$, $pp \rightarrow jj\ell^+\ell^-\bar{\nu}\nu$ and $pp \rightarrow \gamma j\ell^+\ell^-\bar{\nu}\nu$ together. Except for the SM contribution, other processes contributing to background due to detector effects are considered, including $pp \rightarrow (\gamma)\ell\ell + jets$ with missing jets, $pp \rightarrow t\bar{t} \rightarrow jjW^+W^- \rightarrow jj\ell^+\ell^-\bar{\nu}\bar{\nu}$ with b-jets mis-tagged, and $pp \rightarrow j\ell\ell\nu$ with a missing charged lepton.

The datasets are generated using MadGraph5 toolkit[79–84]. To suppress the background with many jets, it is required that the number of jets (N_j) in the final state satisfying

$1 \leq N_j \leq 6$. Because of the presence of neutrinos, it is required that the transverse missing energy (\cancel{E}_T) satisfying $\cancel{E}_T > 200$ GeV. Except for that, the final state is required to have exactly two opposite charged leptons.

	v^1	v^2	v^3	v^4	v^5	v^6	
observables	E_{j_1}	$p_{j_1}^T$	E_{j_2}	$p_{j_2}^T$	E_{ℓ^+}	$p_{\ell^+}^T$	
	v^7	v^8	v^9	v^{10}	v^{11}	v^{12}	v^{13}
observables	E_{ℓ^-}	$p_{\ell^-}^T$	E_γ	p_γ^T	\cancel{E}_T	f_{ℓ^+}	f_{ℓ^-}

TABLE I. The components of the feature space and the corresponding observables.

As a ML algorithm, instead of analyzing the kinematics, we simply chose some typical observables arbitrarily, i.e., the energies (E) and transverse momenta (p^T) of the final state particles are picked as the features. To better utilize the Hilbert space, the f_{ℓ^\pm} are added which are the flavors of charged leptons ($f_{\ell^\pm} = 0, 1$ for electron or muon). In summary, an event is mapped into a 13-dimensional vector \vec{v} whose components are listed in Table I. If there are no photons or less than three jets, the corresponding v^i is set to be zero. The training dataset is $\{\vec{x}_m\}$, where \vec{x} is \vec{v} after z-score standardization [85]. \vec{x}_m is mapped to,

$$|\psi_m\rangle = \frac{1}{\sqrt{1 + \sum_j (x_m^j)^2}} \left(|0\rangle + \sum_{j=1}^7 (x_m^{2j-1} + x_m^{2j}i) |j\rangle \right), \quad (2)$$

where $x_m^j = 0$ with $j > 13$. In the following, $d = 8$ and $d' = 13$ are dimensions of complex and real vectors.

The training dataset has $N = 65536$ events, which can be stored in $n_q = 19$ qubits. We use the ‘hardware efficient’ ansatz [86] with the ‘shifted-circular-alternating’ entanglement layer [87], which is shown in Fig. 1. (d). The circuits are simulated using QuEST [88]. Given that d is small, we do not employ the amplitude amplification, therefore the cc is about $((2 + 3l)n_q + 2(2d - \log_2(d) - 2))cd$ for a test event. If the cc of VQSN is to be less than that of its KNN counterpart (which is $d'N = 8.5 \times 10^5$), $l \leq 17$. In this work, we consider three cases, $l = 5, 10, \text{ and } 15$. As a comparison, we consider (t-)KNN with $K = 1, 10, 100,$ and 1000 , with neighbors determined using Euclidean distance.

After scanning the interval $|f_0| \leq 0.2 \text{ TeV}^{-4}$, the cross-section after event selection is fitted according to a bilinear function $\sigma(f_0) = \sigma_{\text{bg}} + f_0\sigma_{\text{int}} + f_0^2\sigma_{\text{NP}}$. The expected coefficient constraints can be estimated using the signal significance ($\mathcal{S}_{\text{stat}}$) [89]. The tunable

		\mathcal{S}_{stat}		
		2	3	5
QSN		[-0.068, 0.065]	[-0.083, 0.081]	[-0.108, 0.106]
VQSN	l			
	5	[-0.063, 0.057]	[-0.077, 0.071]	[-0.101, 0.095]
	10	[-0.057, 0.049]	[-0.070, 0.063]	[-0.094, 0.086]
	15	[-0.053, 0.046]	[-0.066, 0.059]	[-0.089, 0.082]
KNN	k			
	1	[-0.084, 0.078]	[-0.102, 0.097]	[-0.132, 0.126]
	10	[-0.076, 0.071]	[-0.093, 0.088]	[-0.120, 0.115]
	100	[-0.075, 0.070]	[-0.092, 0.086]	[-0.118, 0.113]
	1000	[-0.068, 0.064]	[-0.084, 0.079]	[-0.108, 0.104]
t-KNN	K			
	10	[-0.056, 0.055]	[-0.069, 0.067]	[-0.090, 0.088]
	100	[-0.039, 0.038]	[-0.048, 0.047]	[-0.064, 0.063]
	1000	[-0.031, 0.031]	[-0.039, 0.039]	[-0.053, 0.053]

TABLE II. The expected constraints on the f_0 at $\sqrt{s} = 13$ TeV, $L = 137 \text{ fb}^{-1}$ and $\mathcal{S}_{stat} = 2, 3,$ and 5 using different event selection strategies.

parameters \hat{a}_{th} and \hat{b}_{th} are chosen to maximize \mathcal{S}_{stat} . For optimal \hat{a}_{th} and \hat{b}_{th} , the expected constraints at the 13 TeV LHC with $L = 137 \text{ fb}^{-1}$ are listed in Table II. The results indicate that the constraints obtained by various algorithms are at a same order of magnitude. t-KNN ($K = 1000$) is the most effective, followed by t-KNN ($K = 100$), VQSN ($l = 15$), and VQSN ($l = 10$), which demonstrate tighter constraints compared with Ref. [71]. This suggests that the processes under consideration are sensitive to the gQGCs and are worth of consideration in the global fit. It is evident that the constraints obtained by VQSN are more off-centered, indicating that the contribution of the interference is more preserved, which may confer an advantage when the coefficient is in a more stringent region as the luminosity increases.

We use the average success rate of background events to estimate the cc. The requisite number of quantum gates is presented in Table III. The single qubit gates are combined as

	QSN	VQSN			(t-)KNN
l		5	10	15	
U	914865	311	201	296	
CZ	0	95	190	285	
CNOT	917506	8	8	8	
total	1832371	209	399	589	
cc	9.9×10^8	8.5×10^4	1.6×10^5	2.4×10^5	8.5×10^5
depth	1832354	105	210	315	

TABLE III. The number of single qubit gates, two qubit gates used in (V)QSN event selection strategies. The ‘total’ represents the number of gates to measure the classification assignment once for one test vector. The depths of circuits are also listed.

the single-qubit unitary gates (U). It can be seen that the cc for VQSN is less than that of (t-)KNN, especially for $l = 5$ where cc is reduced by an order of magnitude. This indicates that even with classical data, VQSN can still be more efficient. Note that, the superiority of VQSN can be even further evident for a larger N or a larger d . The depth of the quantum circuit is another significant metric. For VQSN, the depth is less than or equal to $r_{ans} + r_{ae}$ with $r_{ans} = (q + 1)l + 1$ and $r_{ae} = 4d - 3 - 4 \log_2(d)$ are the depths of the ansatz and inverse of amplitude encode, respectively.

V. SUMMARY

In this study, we present a novel VQSN algorithm for classification. We use VQSN to study gQGCs at the LHC using in processes $pp \rightarrow jj\ell^+\ell^-\nu\bar{\nu}$, $pp \rightarrow j\ell^+\ell^-\nu\bar{\nu}$ and $pp \rightarrow \gamma j\ell^+\ell^-\nu\bar{\nu}$. These processes can be concluded to be sensitive to the gQGCs. The expected coefficient constraints are of a same magnitude to those obtained in the $pp \rightarrow \gamma\gamma$ process [71]. Consequently, they can serve as a valuable supplement to the constraints on the gQGCs. Moreover, the $pp \rightarrow jj\ell^+\ell^-\nu\bar{\nu}$ process contains a vector boson scattering process which is expected to be more significant at higher energies [90], therefore is expected to be more important at future colliders. It is noteworthy that, as an ML algorithm, VQSN does not require the analysis of the kinematic characteristics and its usability should be independent

of the operator being searched and can be applied in future studies of other NP models.

In terms of cc , the VQSN is capable of achieving the same order of magnitude of the discriminative power to that of the KNN, while requiring less cc . It is important to note that the datasets are classical, i.e., even when working with classical data, the VQSN can demonstrate its superiority in efficiency. Since the larger training dataset and the larger feature space, the more efficient the VQSN is, the significance of VQSN is likely to increase as the processes under consideration become more intricate.

This study has not addressed further improvements such as encoding the dataset using a nonlinear approach [91]. It is also possible to utilize the vast Hilbert space of quantum computers to separate the signal from the background more when mapping to the quantum feature space [92]. Furthermore, it would be beneficial to investigate the simulation of the collision process on a quantum computer. Both QSN and VQSN could be employed as a part of the simulation which are able to process data directly from a quantum computer. In conclusion, QSN and VQSN are suitable for the NP phenomenological study.

ACKNOWLEDGMENTS

This work was supported in part by the National Natural Science Foundation of China under Grants Nos. 11875157 and 12147214, and the Natural Science Foundation of the Liaoning Scientific Committee No. LJKZ0978.

-
- [1] Y. Farzan and M. Tortola, Neutrino oscillations and Non-Standard Interactions, *Front. in Phys.* **6**, 10 (2018), [arXiv:1710.09360 \[hep-ph\]](#).
 - [2] *Neutrino Non-Standard Interactions: A Status Report*, Vol. 2 (2019) [arXiv:1907.00991 \[hep-ph\]](#).
 - [3] C. A. Argüelles *et al.*, Snowmass white paper: beyond the standard model effects on neutrino flavor: Submitted to the proceedings of the US community study on the future of particle physics (Snowmass 2021), *Eur. Phys. J. C* **83**, 15 (2023), [arXiv:2203.10811 \[hep-ph\]](#).
 - [4] T. Aaltonen *et al.* (CDF), High-precision measurement of the W boson mass with the CDF II detector, *Science* **376**, 170 (2022).

- [5] J. de Blas, M. Pierini, L. Reina, and L. Silvestrini, Impact of the Recent Measurements of the Top-Quark and W-Boson Masses on Electroweak Precision Fits, *Phys. Rev. Lett.* **129**, 271801 (2022), [arXiv:2204.04204 \[hep-ph\]](#).
- [6] B. Abi *et al.* (Muon g-2), Measurement of the Positive Muon Anomalous Magnetic Moment to 0.46 ppm, *Phys. Rev. Lett.* **126**, 141801 (2021), [arXiv:2104.03281 \[hep-ex\]](#).
- [7] D. P. Aguillard *et al.* (Muon g-2), Measurement of the Positive Muon Anomalous Magnetic Moment to 0.20 ppm, *Phys. Rev. Lett.* **131**, 161802 (2023), [arXiv:2308.06230 \[hep-ex\]](#).
- [8] T. Aoyama *et al.*, The anomalous magnetic moment of the muon in the Standard Model, *Phys. Rept.* **887**, 1 (2020), [arXiv:2006.04822 \[hep-ph\]](#).
- [9] A. Crivellin and B. Mellado, Anomalies in Particle Physics (2023) [arXiv:2309.03870 \[hep-ph\]](#).
- [10] J. Ellis, Outstanding questions: Physics beyond the Standard Model, *Phil. Trans. Roy. Soc. Lond. A* **370**, 818 (2012).
- [11] V. Innocente, Y. F. Wang, and Z. P. Zhang, Identification of tau decays using a neural network, *Nucl. Instrum. Meth. A* **323**, 647 (1992).
- [12] K. Albertsson *et al.*, Machine Learning in High Energy Physics Community White Paper, *J. Phys. Conf. Ser.* **1085**, 022008 (2018), [arXiv:1807.02876 \[physics.comp-ph\]](#).
- [13] D. Guest, K. Cranmer, and D. Whiteson, Deep Learning and its Application to LHC Physics, *Ann. Rev. Nucl. Part. Sci.* **68**, 161 (2018), [arXiv:1806.11484 \[hep-ex\]](#).
- [14] A. Radovic, M. Williams, D. Rousseau, M. Kagan, D. Bonacorsi, A. Himmel, A. Aurisano, K. Terao, and T. Wongjirad, Machine learning at the energy and intensity frontiers of particle physics, *Nature* **560**, 41 (2018).
- [15] P. Baldi, P. Sadowski, and D. Whiteson, Searching for Exotic Particles in High-Energy Physics with Deep Learning, *Nature Commun.* **5**, 4308 (2014), [arXiv:1402.4735 \[hep-ph\]](#).
- [16] J. Ren, L. Wu, J. M. Yang, and J. Zhao, Exploring supersymmetry with machine learning, *Nucl. Phys. B* **943**, 114613 (2019), [arXiv:1708.06615 \[hep-ph\]](#).
- [17] M. Abdughani, J. Ren, L. Wu, and J. M. Yang, Probing stop pair production at the LHC with graph neural networks, *JHEP* **08**, 055, [arXiv:1807.09088 \[hep-ph\]](#).
- [18] J. Ren, L. Wu, and J. M. Yang, Unveiling CP property of top-Higgs coupling with graph neural networks at the LHC, *Phys. Lett. B* **802**, 135198 (2020), [arXiv:1901.05627 \[hep-ph\]](#).
- [19] M. Letizia, G. Losapio, M. Rando, G. Grosso, A. Wulzer, M. Pierini, M. Zanetti, and L. Rosasco, Learning new physics efficiently with nonparametric methods, *Eur. Phys. J. C*

- 82**, 879 (2022), [arXiv:2204.02317 \[hep-ph\]](#).
- [20] R. T. D’Agnolo, G. Grosso, M. Pierini, A. Wulzer, and M. Zanetti, Learning multivariate new physics, *Eur. Phys. J. C* **81**, 89 (2021), [arXiv:1912.12155 \[hep-ph\]](#).
- [21] R. T. D’Agnolo and A. Wulzer, Learning New Physics from a Machine, *Phys. Rev. D* **99**, 015014 (2019), [arXiv:1806.02350 \[hep-ph\]](#).
- [22] J.-C. Yang, J.-H. Chen, and Y.-C. Guo, Extract the energy scale of anomalous $\gamma\gamma \rightarrow W^+W^-$ scattering in the vector boson scattering process using artificial neural networks, *JHEP* **09**, 085, [arXiv:2107.13624 \[hep-ph\]](#).
- [23] J.-C. Yang, X.-Y. Han, Z.-B. Qin, T. Li, and Y.-C. Guo, Measuring the anomalous quartic gauge couplings in the $W^+W^- \rightarrow W^+W^-$ process at muon collider using artificial neural networks, *JHEP* **09**, 074, [arXiv:2204.10034 \[hep-ph\]](#).
- [24] A. De Simone and T. Jacques, Guiding New Physics Searches with Unsupervised Learning, *Eur. Phys. J. C* **79**, 289 (2019), [arXiv:1807.06038 \[hep-ph\]](#).
- [25] J.-C. Yang, Y.-C. Guo, and L.-H. Cai, Using a nested anomaly detection machine learning algorithm to study the neutral triple gauge couplings at an $e+e-$ collider, *Nucl. Phys. B* **977**, 115735 (2022), [arXiv:2111.10543 \[hep-ph\]](#).
- [26] J. Lee, N. Chanon, A. Levin, J. Li, M. Lu, Q. Li, and Y. Mao, Polarization fraction measurement in same-sign WW scattering using deep learning, *Phys. Rev. D* **99**, 033004 (2019), [arXiv:1812.07591 \[hep-ph\]](#).
- [27] M. A. Md Ali, N. Badrud’din, H. Abdullah, and F. Kemi, Alternate methods for anomaly detection in high-energy physics via semi-supervised learning, *Int. J. Mod. Phys. A* **35**, 2050131 (2020).
- [28] E. Fol, R. Tomás, J. Coello de Portugal, and G. Franchetti, Detection of faulty beam position monitors using unsupervised learning, *Phys. Rev. Accel. Beams* **23**, 102805 (2020).
- [29] G. Kasieczka *et al.*, The LHC Olympics 2020 a community challenge for anomaly detection in high energy physics, *Rept. Prog. Phys.* **84**, 124201 (2021), [arXiv:2101.08320 \[hep-ph\]](#).
- [30] L. Jiang, Y.-C. Guo, and J.-C. Yang, Detecting anomalous quartic gauge couplings using the isolation forest machine learning algorithm, *Phys. Rev. D* **104**, 035021 (2021), [arXiv:2103.03151 \[hep-ph\]](#).
- [31] Y.-F. Dong, Y.-C. Mao, and J.-C. Yang, Searching for anomalous quartic gauge couplings at muon colliders using principal component analysis, *Eur. Phys. J. C* **83**, 555 (2023),

- [arXiv:2304.01505 \[hep-ph\]](#).
- [32] M. Crispim Romão, N. F. Castro, and R. Pedro, Finding New Physics without learning about it: Anomaly Detection as a tool for Searches at Colliders, *Eur. Phys. J. C* **81**, 27 (2021), [Erratum: *Eur.Phys.J.C* 81, 1020 (2021)], [arXiv:2006.05432 \[hep-ph\]](#).
- [33] M. van Beekveld, S. Caron, L. Hendriks, P. Jackson, A. Leinweber, S. Otten, R. Patrick, R. Ruiz De Austri, M. Santoni, and M. White, Combining outlier analysis algorithms to identify new physics at the LHC, *JHEP* **09**, 024, [arXiv:2010.07940 \[hep-ph\]](#).
- [34] M. Kuusela, T. Vatanen, E. Malmi, T. Raiko, T. Aaltonen, and Y. Nagai, Semi-Supervised Anomaly Detection - Towards Model-Independent Searches of New Physics, *J. Phys. Conf. Ser.* **368**, 012032 (2012), [arXiv:1112.3329 \[physics.data-an\]](#).
- [35] Y.-T. Zhang, X.-T. Wang, and J.-C. Yang, Searching for gluon quartic gauge couplings at muon colliders using the autoencoder, *Phys. Rev. D* **109**, 095028 (2024), [arXiv:2311.16627 \[hep-ph\]](#).
- [36] S. Zhang, J.-C. Yang, and Y.-C. Guo, Using k-means assistant event selection strategy to study anomalous quartic gauge couplings at muon colliders, *Eur. Phys. J. C* **84**, 142 (2024), [arXiv:2302.01274 \[hep-ph\]](#).
- [37] Z. Chen, K. J. Satzinger, J. Atalaya, A. N. Korotkov, A. Dunsworth, D. Sank, C. Quintana, M. McEwen, R. Barends, P. V. Klimov, S. Hong, C. Jones, A. Petukhov, D. Kafri, S. Demura, B. Burkett, C. Gidney, A. G. Fowler, A. Paler, H. Putterman, I. Aleiner, F. Arute, K. Arya, R. Babbush, J. C. Bardin, A. Bengtsson, A. Bourassa, M. Broughton, B. B. Buckley, D. A. Buell, N. Bushnell, B. Chiaro, R. Collins, W. Courtney, A. R. Derk, D. Eppens, C. Erickson, E. Farhi, B. Foxen, M. Giustina, A. Greene, J. A. Gross, M. P. Harrigan, S. D. Harrington, J. Hilton, A. Ho, T. Huang, W. J. Huggins, L. B. Ioffe, S. V. Isakov, E. Jeffrey, Z. Jiang, K. Kechedzhi, S. Kim, A. Kitaev, F. Kostritsa, D. Landhuis, P. Laptev, E. Lucero, O. Martin, J. R. McClean, T. McCourt, X. Mi, K. C. Miao, M. Mohseni, S. Montazeri, W. Mruczkiewicz, J. Mutus, O. Naaman, M. Neeley, C. Neill, M. Newman, M. Y. Niu, T. E. O'Brien, A. Opremcak, E. Ostby, B. Pató, N. Redd, P. Roushan, N. C. Rubin, V. Shvarts, D. Strain, M. Szalay, M. D. Trevithick, B. Villalonga, T. White, Z. J. Yao, P. Yeh, J. Yoo, A. Zalcman, H. Neven, S. Boixo, V. Smelyanskiy, Y. Chen, A. Megrant, and J. Kelly, Exponential suppression of bit or phase errors with cyclic error correction, *Nature* **595**, 383–387 (2021), [arXiv:2102.06132](#).
- [38] F. Arute *et al.*, Quantum supremacy using a programmable superconducting processor, *Nature*

- 574**, 505 (2019), [arXiv:1910.11333 \[quant-ph\]](#).
- [39] J. Preskill, Quantum Computing in the NISQ era and beyond, *Quantum* **2**, 79 (2018), [arXiv:1801.00862 \[quant-ph\]](#).
- [40] R. P. Feynman, Simulating physics with computers, *Int. J. Theor. Phys.* **21**, 467 (1982).
- [41] A. Roggero and J. Carlson, Dynamic linear response quantum algorithm, *Phys. Rev. C* **100**, 034610 (2019), [arXiv:1804.01505 \[quant-ph\]](#).
- [42] A. Roggero, A. C. Y. Li, J. Carlson, R. Gupta, and G. N. Perdue, Quantum Computing for Neutrino-Nucleus Scattering, *Phys. Rev. D* **101**, 074038 (2020), [arXiv:1911.06368 \[quant-ph\]](#).
- [43] C. W. Bauer *et al.*, Quantum Simulation for High-Energy Physics, *PRX Quantum* **4**, 027001 (2023), [arXiv:2204.03381 \[quant-ph\]](#).
- [44] M. Carena, H. Lamm, Y.-Y. Li, and W. Liu, Improved Hamiltonians for Quantum Simulations of Gauge Theories, *Phys. Rev. Lett.* **129**, 051601 (2022), [arXiv:2203.02823 \[hep-lat\]](#).
- [45] E. J. Gustafson, H. Lamm, F. Lovelace, and D. Musk, Primitive quantum gates for an SU(2) discrete subgroup: Binary tetrahedral, *Phys. Rev. D* **106**, 114501 (2022), [arXiv:2208.12309 \[quant-ph\]](#).
- [46] H. Lamm, Y.-Y. Li, J. Shu, Y.-L. Wang, and B. Xu, Block encodings of discrete subgroups on a quantum computer, *Phys. Rev. D* **110**, 054505 (2024), [arXiv:2405.12890 \[hep-lat\]](#).
- [47] M. Carena, H. Lamm, Y.-Y. Li, and W. Liu, Quantum error thresholds for gauge-redundant digitizations of lattice field theories, *Phys. Rev. D* **110**, 054516 (2024), [arXiv:2402.16780 \[hep-lat\]](#).
- [48] Y. Y. Atas, J. Zhang, R. Lewis, A. Jahanpour, J. F. Haase, and C. A. Muschik, SU(2) hadrons on a quantum computer via a variational approach, *Nature Commun.* **12**, 6499 (2021), [arXiv:2102.08920 \[quant-ph\]](#).
- [49] Y.-Y. Li, M. O. Sajid, and J. Unmuth-Yockey, Lattice holography on a quantum computer, *Phys. Rev. D* **110**, 034507 (2024), [arXiv:2312.10544 \[hep-lat\]](#).
- [50] X. Cui, Y. Shi, and J.-C. Yang, Circuit-based digital adiabatic quantum simulation and pseudoquantum simulation as new approaches to lattice gauge theory, *JHEP* **08**, 160, [arXiv:1910.08020 \[quant-ph\]](#).
- [51] Y.-T. Zou, Y.-J. Bo, and J.-C. Yang, Optimize quantum simulation using a force-gradient integrator, *EPL* **135**, 10004 (2021), [arXiv:2103.05876 \[quant-ph\]](#).
- [52] I. M. Georgescu, S. Ashhab, and F. Nori, Quantum Simulation, *Rev. Mod. Phys.* **86**, 153

- (2014), [arXiv:1308.6253 \[quant-ph\]](#).
- [53] H. Lamm, S. Lawrence, and Y. Yamauchi (NuQS), Parton physics on a quantum computer, *Phys. Rev. Res.* **2**, 013272 (2020), [arXiv:1908.10439 \[hep-lat\]](#).
- [54] T. Li, X. Guo, W. K. Lai, X. Liu, E. Wang, H. Xing, D.-B. Zhang, and S.-L. Zhu (QuNu), Partonic collinear structure by quantum computing, *Phys. Rev. D* **105**, L111502 (2022), [arXiv:2106.03865 \[hep-ph\]](#).
- [55] M. G. Echevarria, I. L. Egusquiza, E. Rico, and G. Schnell, Quantum simulation of light-front parton correlators, *Phys. Rev. D* **104**, 014512 (2021), [arXiv:2011.01275 \[quant-ph\]](#).
- [56] A. Pérez-Salinas, J. Cruz-Martinez, A. A. Alhajri, and S. Carrazza, Determining the proton content with a quantum computer, *Phys. Rev. D* **103**, 034027 (2021), [arXiv:2011.13934 \[hep-ph\]](#).
- [57] S. P. Jordan, K. S. M. Lee, and J. Preskill, Quantum Computation of Scattering in Scalar Quantum Field Theories, *Quant. Inf. Comput.* **14**, 1014 (2014), [arXiv:1112.4833 \[hep-th\]](#).
- [58] N. Mueller, A. Tarasov, and R. Venugopalan, Deeply inelastic scattering structure functions on a hybrid quantum computer, *Phys. Rev. D* **102**, 016007 (2020), [arXiv:1908.07051 \[hep-th\]](#).
- [59] Y. Zhu, W. Zhuang, C. Qian, Y. Ma, D. E. Liu, M. Ruan, and C. Zhou, A Novel Quantum Realization of Jet Clustering in High-Energy Physics Experiments (2024) [arXiv:2407.09056 \[quant-ph\]](#).
- [60] J. Biamonte, P. Wittek, N. Pancotti, P. Rebentrost, N. Wiebe, and S. Lloyd, Quantum machine learning, *Nature* **549**, 195 (2017), [arXiv:1611.09347 \[quant-ph\]](#).
- [61] M. Schuld, I. Sinayskiy, and F. Petruccione, An introduction to quantum machine learning, *Contemporary Physics* **56**, 172 (2015).
- [62] D. P. García, J. Cruz-Benito, and F. J. García-Peñalvo, Systematic Literature Review: Quantum Machine Learning and its applications (2022) [arXiv:2201.04093 \[quant-ph\]](#).
- [63] W. Guan, G. Perdue, A. Pesah, M. Schuld, K. Terashi, S. Vallecorsa, and J.-R. Vlimant, Quantum Machine Learning in High Energy Physics, *Mach. Learn. Sci. Tech.* **2**, 011003 (2021), [arXiv:2005.08582 \[quant-ph\]](#).
- [64] S. L. Wu *et al.*, Application of quantum machine learning using the quantum variational classifier method to high energy physics analysis at the LHC on IBM quantum computer simulator and hardware with 10 qubits, *J. Phys. G* **48**, 125003 (2021), [arXiv:2012.11560 \[quant-ph\]](#).

- [65] E. Grant, M. Benedetti, S. Cao, A. Hallam, J. Lockhart, V. Stojevic, A. G. Green, and S. Severini, Hierarchical quantum classifiers, [npj Quantum Inf. **4**, 65 \(2018\)](#).
- [66] K. Terashi, M. Kaneda, T. Kishimoto, M. Saito, R. Sawada, and J. Tanaka, Event Classification with Quantum Machine Learning in High-Energy Physics, [Comput. Softw. Big Sci. **5**, 2 \(2021\)](#), [arXiv:2002.09935 \[physics.comp-ph\]](#).
- [67] S. L. Wu *et al.*, Application of quantum machine learning using the quantum kernel algorithm on high energy physics analysis at the LHC, [Phys. Rev. Res. **3**, 033221 \(2021\)](#), [arXiv:2104.05059 \[quant-ph\]](#).
- [68] S. Zhang, Y.-C. Guo, and J.-C. Yang, Optimize the event selection strategy to study the anomalous quartic gauge couplings at muon colliders using the support vector machine and quantum support vector machine, [Eur. Phys. J. C **84**, 833 \(2024\)](#), [arXiv:2311.15280 \[hep-ph\]](#).
- [69] A. Fadol, Q. Sha, Y. Fang, Z. Li, S. Qian, Y. Xiao, Y. Zhang, and C. Zhou, Application of quantum machine learning in a Higgs physics study at the CEPC, [Int. J. Mod. Phys. A **39**, 2450007 \(2024\)](#), [arXiv:2209.12788 \[hep-ex\]](#).
- [70] S. Zhang, K.-X. Chen, and J.-C. Yang, Detect anomalous quartic gauge couplings at muon colliders with quantum kernel k-means (2024) [arXiv:2409.07010 \[hep-ph\]](#).
- [71] J. Ellis and S.-F. Ge, Constraining Gluonic Quartic Gauge Coupling Operators with $gg \rightarrow \gamma\gamma$, [Phys. Rev. Lett. **121**, 041801 \(2018\)](#), [arXiv:1802.02416 \[hep-ph\]](#).
- [72] J. Ellis, S.-F. Ge, and K. Ma, Hadron collider probes of the quartic couplings of gluons to the photon and Z boson, [JHEP **04**, 123](#), [arXiv:2112.06729 \[hep-ph\]](#).
- [73] J.-C. Yang, Y.-C. Guo, and Y.-F. Dong, Study of the gluonic quartic gauge couplings at muon colliders (2023) p. 115201, [arXiv:2307.04207 \[hep-ph\]](#).
- [74] S. Weinberg, Baryon and Lepton Nonconserving Processes, [Phys. Rev. Lett. **43**, 1566 \(1979\)](#).
- [75] B. Grzadkowski, M. Iskrzynski, M. Misiak, and J. Rosiek, Dimension-Six Terms in the Standard Model Lagrangian, [JHEP **10**, 085](#), [arXiv:1008.4884 \[hep-ph\]](#).
- [76] S. Willenbrock and C. Zhang, Effective Field Theory Beyond the Standard Model, [Ann. Rev. Nucl. Part. Sci. **64**, 83 \(2014\)](#), [arXiv:1401.0470 \[hep-ph\]](#).
- [77] E. Masso, An Effective Guide to Beyond the Standard Model Physics, [JHEP **10**, 128](#), [arXiv:1406.6376 \[hep-ph\]](#).
- [78] G. Brassard, P. Hoyer, M. Mosca, and A. Tapp, Quantum amplitude amplification and estimation (2000) [arXiv:quant-ph/0005055](#).

- [79] J. Alwall, R. Frederix, S. Frixione, V. Hirschi, F. Maltoni, O. Mattelaer, H. S. Shao, T. Stelzer, P. Torrielli, and M. Zaro, The automated computation of tree-level and next-to-leading order differential cross sections, and their matching to parton shower simulations, *JHEP* **07**, 079, [arXiv:1405.0301 \[hep-ph\]](#).
- [80] N. D. Christensen and C. Duhr, FeynRules - Feynman rules made easy, *Comput. Phys. Commun.* **180**, 1614 (2009), [arXiv:0806.4194 \[hep-ph\]](#).
- [81] C. Degrande, C. Duhr, B. Fuks, D. Grellscheid, O. Mattelaer, and T. Reiter, UFO - The Universal FeynRules Output, *Comput. Phys. Commun.* **183**, 1201 (2012), [arXiv:1108.2040 \[hep-ph\]](#).
- [82] T. Sjöstrand, S. Ask, J. R. Christiansen, R. Corke, N. Desai, P. Ilten, S. Mrenna, S. Prestel, C. O. Rasmussen, and P. Z. Skands, An introduction to PYTHIA 8.2, *Comput. Phys. Commun.* **191**, 159 (2015), [arXiv:1410.3012 \[hep-ph\]](#).
- [83] J. de Favereau, C. Delaere, P. Demin, A. Giammanco, V. Lemaître, A. Mertens, and M. Selvaggi (DELPHES 3), DELPHES 3, A modular framework for fast simulation of a generic collider experiment, *JHEP* **02**, 057, [arXiv:1307.6346 \[hep-ex\]](#).
- [84] Y.-C. Guo, F. Feng, A. Di, S.-Q. Lu, and J.-C. Yang, MLAnalysis: An open-source program for high energy physics analyses, *Comput. Phys. Commun.* **294**, 108957 (2024), [arXiv:2305.00964 \[hep-ph\]](#).
- [85] D. Donoho and J. Jin, Higher criticism for detecting sparse heterogeneous mixtures, *The Annals of Statistics* **32**, 10.1214/009053604000000265 (2004).
- [86] A. Kandala, A. Mezzacapo, K. Temme, M. Takita, M. Brink, J. M. Chow, and J. M. Gambetta, Hardware-efficient variational quantum eigensolver for small molecules and quantum magnets, *Nature* **549**, 242 (2017), [arXiv:1704.05018 \[quant-ph\]](#).
- [87] S. Sim, P. D. Johnson, and A. Aspuru-Guzik, Expressibility and Entangling Capability of Parameterized Quantum Circuits for Hybrid Quantum-Classical Algorithms, *Adv. Quantum Technol.* **2**, 1900070 (2019), [arXiv:1905.10876 \[quant-ph\]](#).
- [88] T. Jones, A. Brown, I. Bush, and S. C. Benjamin, QuEST and High Performance Simulation of Quantum Computers, *Sci. Rep.* **9**, 10736 (2019).
- [89] P. A. Zyla *et al.* (Particle Data Group), Review of Particle Physics, *PTEP* **2020**, 083C01 (2020).
- [90] J.-C. Yang, Z.-B. Qing, X.-Y. Han, Y.-C. Guo, and T. Li, Tri-photon at muon collider: a new

- process to probe the anomalous quartic gauge couplings, [JHEP **22**, 053](#), [arXiv:2204.08195 \[hep-ph\]](#).
- [91] V. Havlicek, A. D. Córcoles, K. Temme, A. W. Harrow, A. Kandala, J. M. Chow, and J. M. Gambetta, Supervised learning with quantum-enhanced feature spaces, [Nature **567**, 209 \(2019\)](#), [arXiv:1804.11326 \[quant-ph\]](#).
- [92] S. Lloyd, M. Schuld, A. Ijaz, J. Izaac, and N. Killoran, Quantum embeddings for machine learning (2020) [arXiv:2001.03622 \[quant-ph\]](#).